LASER INTERFEROMETER GRAVITATIONAL WAVE OBSERVATORY

- LIGO -

CALIFORNIA INSTITUTE OF TECHNOLOGY
MASSACHUSETTS INSTITUTE OF TECHNOLOGY

Technical Note	LIGO-T980044-06	-E	99.06.25
Document	*Doc Number*	*Group*	*Date*

Determination of Global and Local Coordinate Axes for the LIGO Sites

Title

William Althouse
Larry Jones
Albert Lazzarini

Author[s]

This is an internal working note of
the LIGO Project

California Institute of Technology
LIGO Project - MS 18-33
Pasadena CA 91125
Phone +1.626.395.2966
Fax +1.626.304.9834
E-mail: info@ligo.caltech.edu

Massachusetts Institute of Technology
LIGO Project - MS 20B-145
Cambridge, MA 01239
Phone +1.617.253.4824
Fax +1.617.253.7014
E-mail: info@ligo.mit.edu

WWW: http://www.ligo.caltech.edu

Table of Contents

1 Purpose 4
2 Hanford Survey Data 5
2.1 Fit to the Survey Data 9
2.2 Error propagators in the fits 13
2.3 Hanford Local Coordinate Systems in each station 17
3 Livingston Survey Data 18
3.1 Fit to the Survey Data 23
3.2 Error propagators in the fits 29
3.3 Livingston Local Coordinate Systems in each station 35
3.4 Positions of LIGO Primary GPS Monuments in the Global Coordinate System 36
4 Graphical representations of the interferometer planes for each site 38

List of Figures

Figure 1: Geodetic and Earth-Fixed Coordinates 9
Figure 2: Scatter plots of fit residuals in plane normal to global axis for Hanford, WA. 12
Figure 3: Dependence of residuals on distance along the arms, Hanford, WA 12
Figure 4: Pitch, yaw, and roll axes for the orientation error analysis. 13
Figure 5: Scatter plots of fit residuals in plane normal to global axis for Livingston, LA 28
Figure 6: Dependence of residuals on distance along the arms for Livingston, LA. 28
Figure 7: Layout of the CB&I control points and primary GPS monument array at Livingston. Dots (colored) denote the CB&I control points for alignment of the beam tubes; plus signs denote the primary GPS monuments. 37
Figure 8: Representation of the interferometer plane inclinations at the two LIGO sites. 39

List of Tables

Table 1: Relevant, Previously Released LIGO Documents 4
Table 2: Design values of the global coordinate positions of BT/VE interface markers 5
Table 3: Cardinal Marker Survey Data for Hanford 6
Table 4: Parameters resulting from best fit to the survey data for Hanford, WA 10
Table 5: Global coordinate positions of as-built BT/VE interface markers 11
Table 6: Sensitivity matrix for the XG coordinate for BTVE markers 14
Table 7: Sensitivity matrix for the YG coordinate for BTVE markers 15
Table 8: Sensitivity matrix for the ZG coordinate for BTVE markers 16
Table 9: Uncertainties in fitted parameters. Changing the best fit values by these amounts result in a doubling of the RMS residual fitting error. 17
Table 10: Hanford Vertex Global-Local System Direction Cosines 17
Table 11: Hanford X End Station (d= 4000m) Global-Local System Direction Cosines 17
Table 12: Hanford Y End Station (d= 4000m) Global-Local System Direction Cosines 18
Table 13: Hanford X Mid-Station (d = 2000m) Global-Local System Direction Cosines 18
Table 14: Hanford Y Mid-Station (d = 2000m) Global-Local System Direction Cosines 18
Table 15: Design values of the global coordinate positions of BT/VE interface markers 19
Table 16: Cardinal Marker Survey Data for Livingston 20
Table 17: Control Point CB&I Survey Data 22

Table 18: Parameters resulting from best fit to the survey data for Livingston, LA 24
Table 19: Global coordinate positions of as-built BT/VE interface markers.....25
Table 20: Global coordinate positions of CB&I control points, meters 26
Table 21: Sensitivity matrix for the XG coordinate for control points.....29
Table 22: Sensitivity matrix for the YG coordinate for control points.....31
Table 23: Sensitivity matrix for the ZG coordinate for control points 33
Table 24: Uncertainties in fitted parameters. Changing the best fit values by these amounts result in a doubling of the RMS residual fitting error.....35
Table 25: Livingston Vertex Global-Local System Direction Cosines 35
Table 26: Livingston X End Station (d= 4000m) Global-Local System Direction Cosines..35
Table 27: Livingston Y End Station (d= 4000m) Global-Local System Direction Cosines..36
Table 28: Report Geodetic Coordinates for the GPS primary monuments at Livingston 36
Table 29: Position of the GPS primary monuments in the site global coordinate system.....38

1 PURPOSE

This document uses survey data taken during the course of fabricating the beam tubes at the LIGO Observatories to determine the as-built orientation and origin for the LIGO Site Coordinate Axes.

Table 1 lists previously issued documents that contain relevant information. The present document supersedes previously released determinations of the coordinate axes because more information is now known about the as-built beam tube and marker geometry. Some earlier analyses used a spherical earth model. At that time, the rough data that were available could be adequately described; later, higher precision GPS data dictated switching to the accepted WGS-84 ellipsoidal model of the earth for refined analyses.

Table 1: Relevant, Previously Released LIGO Documents

LIGO Document umber	*Title*	*Description*
L950128	LIGO Coordinate System	Gives an operational definition of the site global and local coordinate axes
T950004	Derivation of Global and Local Coordinate Axes for the LIGO Sites	Takes the operational definition and derives the *design* beam centerline direction cosines, global and local coordinate axes. Uses a spherical model for the earth and Parsons-provided rough grading survey data.
T950107	Orientation of the LIGO Beam Center Lines with respect to foundation slabs	Written for PSI (the VE contractor) to document the angular deviation from local horizontal of the *design* beam tube centerlines in each of the LIGO stations. Uses data appearing in T950004 (i.e. spherical earth model).
T960176	Determination of the LIGO Global Coordinate Axes for Hanford, WA: final analysis of the LIGO BT/VE interface survey monuments.	Reports the results to a first best-fit determination of the plane defined by the eight cardinal points for the Hanford site. Uses early survey data from RSI and IMTEC. Results are superseded by present, more thorough, document.
D950021	LIGO Arm Layout	Drawing showing BT/VE interface locations
C962080	TDM 014C to CB&I	Provides the height offsets above the marker elevations for establishing the beam tube centerlines at Hanford.

Table 1: Relevant, Previously Released LIGO Documents

LIGO Document umber	*Title*	*Description*
C982209	Livingston Beam Tube Alignment Data	Provides the CB&I control point data for the arm alignment.
C971830-00 C972035-00 C980026-00,-A	LIGO to CB&I Technical Direction Memoranda	Provide survey and design information to CB&I regarding beam line offsets w.r.t BT/VE interface markers
C982063-00	Report on Final Results of the Location of the BT/VE Monuments at the Livingston, Louisiana LIGO Laboratory	Provides the JSB data for the Livingston BT/VE interface markers.
SJB Drawing	LIGO Monuments for LIGO Drawn: 5 August 1997 Signed (by Teegarden): 19 September 1997	Depicts layout of the array of GPS primary monuments: gives latitude, longitude and orthometric height in feet.

2 HANFORD SURVEY DATA

In the course of laying out the Hanford site, eight cardinal points were surveyed in preparation for fabrication and alignment of the beam tubes. These points defined the interface positions for the beam tube (BT) and vacuum equipment (VE) contracts. These points are identified by suitably inscribed marks on each of eight brass markers, denoted {BT/VE1, ..., BT/VE8} (see D950021 for specifications). The design positions in global coordinates of the interface markers are given in **Table 2**.

Table 2: Design values of the global coordinate positions of BT/VE interface markers

Marker ID	X_G	Y_G	Z_G
BT/VE 1	0.000	46.000	-1.070[a]
BT/VE 2	0.000	2007.500	-1.070
BT/VE 3	0.000	2027.000	-1.070
BT/VE 4	0.000	3988.500	-1.070
BT/VE 5	46.000	0.000	-1.070
BT/VE 6	2007.500	0.000	-1.070

Table 2: Design values of the global coordinate positions of BT/VE interface markers

Marker ID	X_G	Y_G	Z_G
BT/VE 7	2027.000	0.000	-1.070
BT/VE 8	3988.500	0.000	-1.070

a. The design for the BT centerline was to be 1.070 m above the finished slab.

BT/VE1 - BT/VE4 lie along the Y arm and BT/VE5 - BT/VE8 are similarly arranged along the X arm.

During the course of constructing the beam tubes, the markers were surveyed a number of times by different parties. Sometimes only a subset of the full three-dimensional position of the markers were determined (e.g., height only). In making use of all data, missing information has been substituted using complementary information from other surveys (e.g., height-only data were augmented with $\{\phi, \lambda\}$ data from other measurements). This will tend to artificially tighten the scatter in the those coordinate directions which are affected by the repeated use of the same $\{\phi, \lambda\}$ coordinates; however, this approach allows all height data to be used. This is desirable because height determinations were typically the noisiest and having more measurements serves to improve the level of precision of the dataset as a whole.

Table 3 presents the survey results for the eight BT/VE markers. The markers were placed on the as-built beam tube slabs. Their heights are affected by slight irregularities in the slab finish. After the first survey by IMTEC and RSI, LIGO determined the best estimate (at that time) for the vertical offsets above each of the markers where the beam tube centerline should be located. The last column in the table shows these vertical offsets. The global coordinate axes were determined by fitting to a beam tube centerline going through points at the indicated offsets above the markers. In reporting the marker locations, the offsets were then subtracted from the residuals to the fit in order to refer the monument locations on the slab surfaces.

Table 3: Cardinal Marker Survey Data for Hanford

Marker ID *Source*	*Latitude[N]*			*Longitude[W}*			*Ellipsoidal height of marker*	*Design height of beam centerline above marker elevation*
	°	′	″	°	′	″	*m*	*m*
BT/VE1								
IMTEC RSI-GroundLoop RSI-GPS CBI-GPS (all same)	46	27	17.65230	-119	24	29.30959	141.4980	1.0602

Table 3: Cardinal Marker Survey Data for Hanford

Marker ID *Source*	*Latitude[N]*			*Longitude[W}*			*Ellipsoidal height of marker*	*Design height of beam centerline above marker elevation*
	°	′	″	°	′	″	*m*	*m*
BT/VE2								
IMTEC	46	26	40.30783	-119	25	43.65422	141.8340	1.0612
RSI-Ground Loop	46	26	40.30785	-119	25	43.65410	141.8260	1.0612
RSI-GPS	46	26	40.30785	-119	25	43.65410	141.8270	1.0612
CBI-GPS	46	26	40.30783	-119	25	43.65421	141.8390	1.0612
BT/VE3								
IMTEC	46	26	39.93653	-119	25	44.39319	141.8402	1.0612
RSI-Ground Loop	46	26	39.93649	-119	25	44.39314	141.8342	1.0612
RSI-GPS	46	26	39.93649	-119	25	44.39314	141.8310	1.0612
CBI-GPS	46	26	39.93653	-119	25	44.39319	141.8450	1.0612

Table 3: Cardinal Marker Survey Data for Hanford

Marker ID *Source*	*Latitude[N]*			*Longitude[W}*			*Ellipsoidal height of marker*	*Design height of beam centerline above marker elevation*
	°	′	″	°	′	″	*m*	*m*
BT/VE4								
IMTEC	46	26	2.57842	-119	26	58.70927	142.7882	1.0592
RSI-Ground Loop	46	26	2.57842	-119	26	58.70928	142.7932	1.0592
RSI-GPS	46	26	2.57842	-119	26	58.70928	142.7980	1.0592
CBI-GPS	46	26	2.57842	-119	26	58.70928	142.7980	1.0592
BT/VE5								
IMTEC	46	27	19.73298	-119	24	28.83263	141.4677	1.0612
RSI-Ground Loop	46	27	19.73310	-119	24	28.83270	141.4677	1.0612
RSI-GPS	46	27	19.73310	-119	24	28.83270	141.4690	1.0612
CBI-GPS	46	27	19.73298	-119	24	28.83263	141.4650	1.0612
BT/VE6								
IMTEC	46	28	11.12085	-119	25	22.87130	140.5684	1.0569
RSI-Ground Loop	46	28	11.12114	-119	25	22.87150	140.5714	1.0569
RSI-GPS	46	28	11.12114	-119	25	22.87150	140.5650	1.0569
BT/VE7								
IMTEC	46	28	11.63174	-119	25	23.40854	140.5626	1.0579
RSI-Ground Loop	46	28	11.63199	-119	25	23.40886	140.5686	1.0579
RSI-GPS	46	28	11.63199	-119	25	23.40886	140.5600	1.0579
BT/VE8								
IMTEC	46	29	3.01234	-119	26	17.47572	140.2633	1.0632
RSI-Ground Loop	46	29	3.01263	-119	26	17.47612	140.2763	1.0632
RSI-GPS	46	29	3.01263	-119	26	17.47612	140.2640	1.0632
CBI-GPS	46	29	3.01234	-119	26	17.47572	140.2680	1.0632

2.1 Fit to the Survey Data

A *global orthonormal coordinate system* was determined which has its $\hat{x}_G$ and $\hat{y}_G$ axes along best fit lines defined by the markers along the arms. The $\hat{z}_G$ axis is defined by the cross product:

$$\hat{z}_G = \hat{x}_G \times \hat{y}_G .$$

The data of Table 3 were converted to the earth-fixed Cartesian system, $\{\hat{x}_E, \hat{y}_E, \hat{z}_E\}$, used for geodetic work. In this system, $\hat{x}_E$ pierces the earth surface at $\{\phi, \lambda\} = \{000, 000\}$, $\hat{y}_E$ pierces the earth's surface at $\{\phi, \lambda\} = \{000, 090E\}$, and $\hat{z}_E$ pierces the earth's surface at $\{\phi, \lambda\} = \{090N, 000\}$. The relationship between the coordinates of a point $\{h, \phi, \lambda\}$ and $\{X_E, Y_E, Z_E\}$ is depicted in **Figure 1**.

Figure 1: Geodetic and Earth-Fixed Coordinates

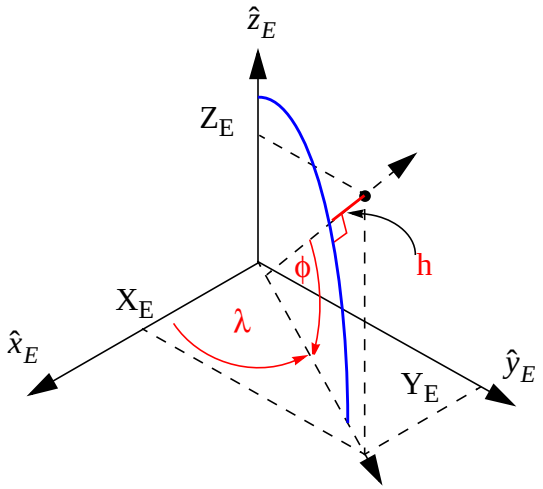

The functional relationships are given by:

$$X_E = ((R[\phi] + h)Cos\phi Cos\lambda$$

$$Y_E = (R[\phi] + h)Cos\phi Sin\lambda$$

$$Z_E = ([1 - \varepsilon^2]R[\phi] + h)Sin\phi$$

The earth model WGS-84, is described by an oblate ellipsoid with its semi-minor axis, b = 6356752.314 m, along $\hat{z}_E$, semi-major axis with value a = 6378137 m, and eccentricity giving $[1 - \varepsilon^2] = 0.993306$. $R[\phi]$ is the local radius of curvature of the ellipsoid at latitude ϕ:

$$R[\phi] = \frac{a^2}{a^2 Cos^2\phi + b^2 Sin^2\phi}$$

Note that in the geodetic model the vector h is aligned along the local surface normal. Consequently its extension to the equatorial plane does not, in general, intersect the origin.

The set of orthonormal axes which best describes the Cartesian data for the markers were determined by a χ^2 minimization of the transverse (2D) residuals of the marker positions from the best-fit axes. There are six degrees of freedom for the fit: 3 translational and three rotational. These were

chosen as:

- **three** coordinates for the vertex, $\{X_v, Y_v, Z_v\}$;
- **two** direction cosines for one axis, $\{n_{xx}, n_{xy}, 1\}$; the z component was fixed.
- **one** direction cosine for the remaining axis (the orientation of the remaining axis in the plane normal to the first axis), $\left\{n_{yx}, \frac{-(n_{xx}n_{yx}+1)}{n_{xy}}, 1\right\}$; this is done by fitting the x component of the second normal, constraining the y and z components.

The errors associated with many of the measured data were not reported in the surveys. Therefore the fitting procedure assumed equal weights for all data: the χ^2 optimization was reduced to a least squares minimization.

The 3-axis RMS residual for the best fit was 0.0053 m. This fit gives parameter values listed in **Figure 4**.

Table 4: Parameters resulting from best fit to the survey data for Hanford, WA

Parameter	*Value*	*Estimated Error*	*Units*
Vertex	Global $\{\hat{x}_G, \hat{y}_G, \hat{z}_G\}$: {0,0,0}	{0.0064, 0.0073, 0.0050}	m
	Geodetic $\{h, \phi, \lambda\}$:{142.554,{46,27,18.528},{-119,24,27.5657}}	-	{m, deg, deg}
	Earth-fixed $\{\hat{x}_E, \hat{y}_E, \hat{z}_E\}$: {-2.1614149 10^6, -3.8346952 10^6, 4.6003502 10^6}	{0.0066, 0.0057, 0.0054}	m
$\hat{x}_G$	Global $\{\hat{x}_G, \hat{y}_G, \hat{z}_G\}$: {1,0,0}	-	
	Earth-fixed $\{\hat{x}_E, \hat{y}_E, \hat{z}_E\}$: {-0.223892, 0.799831, 0.556905}	-	
	Compass Direction: N35.9994° W (ref. geodetic north)[a]	1.93 10^{-6}	radian
	Angle *below* local horizontal at Vertex: 6.195 10^{-4}	2.73 10^{-6}	radian
$\hat{y}_G$	Global $\{\hat{x}_G, \hat{y}_G, \hat{z}_G\}$: {0,1,0}		
	Earth-fixed $\{\hat{x}_E, \hat{y}_E, \hat{z}_E\}$: {-0.913978, 0.0260945, -0.404923}		
	Compass Direction: S54.0006° W (see footnote a)	1.93 10^{-6}	radian
	Angle *above* local horizontal at Vertex: 1.25 10^{-5}	2.73 10^{-6}	radian

Table 4: Parameters resulting from best fit to the survey data for Hanford, WA

Parameter	*Value*	*Estimated Error*	*Units*
$\hat{z}_G$	Global $\{\hat{x}_G, \hat{y}_G, \hat{z}_G\}$: {0,0,1}		
	Earth-fixed $\{\hat{x}_E, \hat{y}_E, \hat{z}_E\}$: {-0.338402,-0.599658,0.725186}		
	Deviation from zenith at vertex: 6.195 10^{-4}, *toward* $\hat{x}_G$	2.73 10^{-6}	radian

a. Site drawings call for arms to run N36.8° W and S53.2° W; these are referred to the WA state plane coordinates (northing & easting). Geodetic north is 47’39” (~0.8 °) W of grid north at the vertex.

Location of as-built BT/VE markers relative to global coordinate system

Using the coordinate system described above, the positions for each of the 8 BT/VE interface markers were determined by averaging the residuals from multiple measurements of individual markers. **Table 5** presents the results.

Table 5: Global coordinate positions of as-built BT/VE interface markers

Marker ID	X_G	Y_G	Z_G
BT/VE 1	0.0000	46.0020	-1.0572
BT/VE 2	-0.0011	2007.5000	-1.0639
BT/VE 3	-0.00052	2027.0000	-1.0642
BT/VE 4	-0.0012	3988.5000	-1.0564
BT/VE 5	45.9970	0.0028	-1.0588
BT/VE 6	2007.5000	0.0010	-1.0585
BT/VE 7	2027.0000	-0.0004	-1.0571
BT/VE 8	3988.5000	-0.0023	-1.0630

The scatter of the residuals is presented graphically in **Figure 2** and **Figure 3**. **Figure 2** presents the scatter in the plane normal to the axis for each arm. There is an apparent greater right-left scatter along the X arm. This is a result of the fact that the best description of the marker positions corresponds to two axes which are not exactly orthogonal: an optimization without imposing the orthogonality constraint between the best fit lines results in axes having an included angle ~ 1.3 microradians greater than 90 degrees. This fact may be seen in the lower panels of **Figure 3** which

present residuals in the horizontal plane as a function of their position along the arms.

Figure 2: Scatter plots of fit residuals in plane normal to global axis for Hanford, WA.

X Arm **Y Arm**

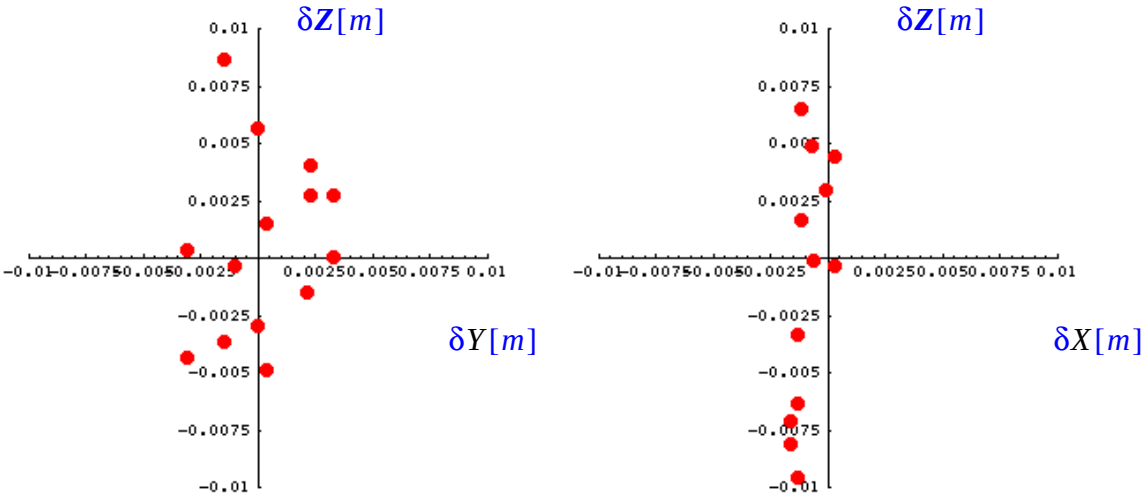

Figure 3: Dependence of residuals on distance along the arms, Hanford, WA.

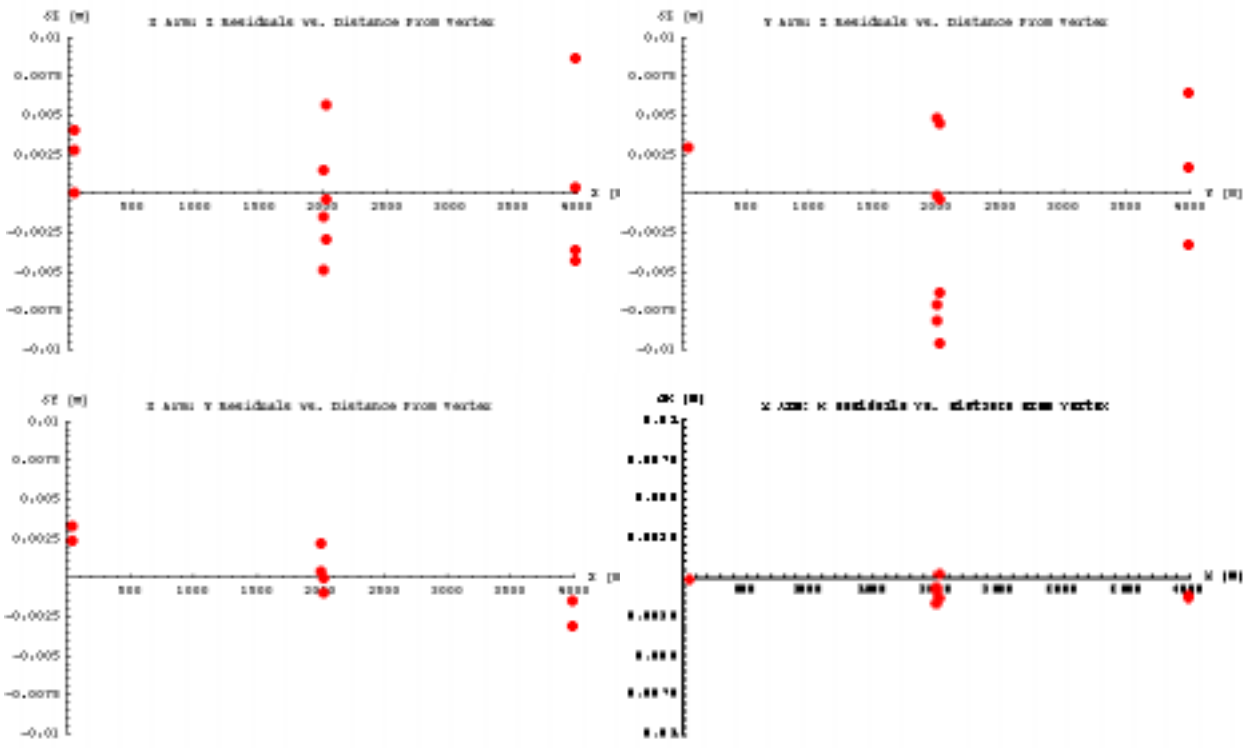

2.2 Error propagators in the fits

Any error in the estimated position of the vertex results in a common mode offset to all marker positions; errors in the estimated directions of the coordinate axis result in either differential mode or common mode offsets according which orientation angle is in error and the effect on marker position is in proportion to marker distances from the vertex. This behavior is represented by the error propagation matrices presented as **Table 6**, **Table 7** and **Table 8**. Each table corresponds to one coordinate. The rows give the effects of parameter variations the eight marker locations. Vertex translational errors are referred along the global axes. Angular errors in the orientation of the axes are referred to roll, pitch and yaw of the $\hat{z}_G$ axis. Pitch gives a common mode up/down displacement for all markers. This rotation is denoted by θ_{CM} which arises from infinitesimal rotational errors about the axis

$$\hat{n}_{CM} = \frac{\hat{y}_G - \hat{x}_G}{\sqrt{2}} \quad ;$$

Yaw gives a differential mode up/down displacement for all markers. This rotation is denoted by θ_{DM} which arises from infinitesimal rotational errors about the axis

$$\hat{n}_{DM} = \frac{\hat{y}_G + \hat{x}_G}{\sqrt{2}}$$

θ_z corresponds to an error in marker positions which arises from infinitesimal rotational errors about the axis $\hat{z}_G$. The roll pitch and yaw axes are depicted in **Figure 4**.

Figure 4: Pitch, yaw, and roll axes for the orientation error analysis.

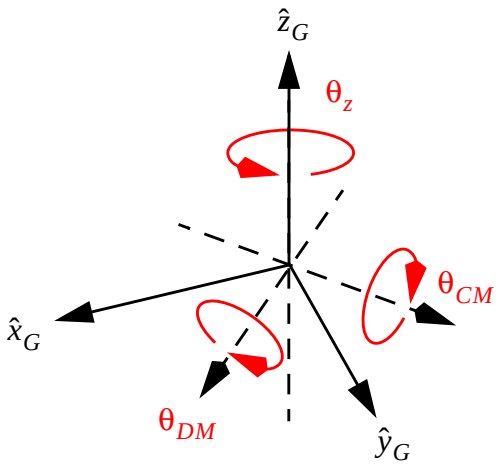

Table 6: Sensitivity matrix for the X_G coordinate for BTVE markers

Marker ID	$\frac{\partial}{\partial V_x}$ [m/m]	$\frac{\partial}{\partial V_y}$ [m/m]	$\frac{\partial}{\partial V_z}$ [m/m]	$\frac{\partial}{\partial \theta_{CM}}$ [m/rad]	$\frac{\partial}{\partial \theta_{DM}}$ [m/rad]	$\frac{\partial}{\partial \theta_z}$ [m/rad]
$BTVE1_x$	-0.224	0.800	0.557	-0.002091	-0.002091	46.002
$BTVE2_x$	-0.224	0.800	0.557	, 0.001873	0.001873	2007.502
$BTVE3_x$	-0.224	0.800	0.557	, 0.002090	0.002090	2027.003
$BTVE4_x$	-0.224	0.800	0.557	-0.001999	-0.001999	3988.504
$BTVE5_x$	-0.224	0.800	0.557	-0.001695	-0.001695	0.00279
$BTVE6_x$	-0.224	0.800	0.557	, 0.001135	0.001135	0.000963
$BTVE7_x$	-0.224	0.800	0.557	-0.0005588	-0.0005588	-0.000356
$BTVE8_x$	-0.224	0.800	0.557	-0.0001960	-0.0001960	-0.00230

Table 7: Sensitivity matrix for the Y_G coordinate for BTVE markers

Marker ID	$\frac{\partial}{\partial V_x}$ [m/m]	$\frac{\partial}{\partial V_y}$ [m/m]	$\frac{\partial}{\partial V_z}$ [m/m]	$\frac{\partial}{\partial \theta_{CM}}$ [m/rad]	$\frac{\partial}{\partial \theta_{DM}}$ [m/rad]	$\frac{\partial}{\partial \theta_z}$ [m/rad]
$BTVE1_y$	-0.914	0.0261	-0.405	-0.002091	0.002091	0.0000426
$BTVE2_y$	-0.914	0.0261	-0.405	0.001873	-0.001873	0.00111
$BTVE3_y$	-0.914	0.0261	-0.405	0.002090	-0.002090	0.000519
$BTVE4_y$	-0.914	0.0261	-0.405	-0.001999	0.001999	0.001217
$BTVE5_y$	-0.914	0.0261	-0.405	-0.001695	0.001695	-45.997
$BTVE6_y$	-0.914	0.0261	-0.405	0.001135	-0.001135	-2007.500
$BTVE7_y$	-0.914	0.0261	-0.405	-0.0005588	0.0005588	-2027.000
$BTVE8_y$	-0.914	0.0261	-0.405	-0.0001960	0.0001960	-3988.497

Table 8: Sensitivity matrix for the Z_G coordinate for BTVE markers

Marker ID	$\frac{\partial}{\partial V_x}$ [m/m]	$\frac{\partial}{\partial V_y}$ [m/m]	$\frac{\partial}{\partial V_z}$ [m/m]	$\frac{\partial}{\partial \theta_{CM}}$ [m/rad]	$\frac{\partial}{\partial \theta_{DM}}$ [m/rad]	$\frac{\partial}{\partial \theta_z}$ [m/rad]
$BTVE1_z$	-0.338	-0.600	0.725	32.528	-32.528	0
$BTVE2_z$	-0.338	-0.600	0.725	1419.517	-1419.519	0
$BTVE3_z$	-0.338	-0.600	0.725	1433.307	-1433.308	0
$BTVE4_z$	-0.338	-0.600	0.725	2820.298	-2820.299	0
$BTVE5_z$	-0.338	-0.600	0.725	32.527	32.523	0
$BTVE6_z$	-0.338	-0.600	0.725	1419.517	1419.516	0
$BTVE7_z$	-0.338	-0.600	0.725	1433.305	1433.306	0
$BTVE8_z$	-0.338	-0.600	0.725	2820.291	2820.295	0

Table 9 presents uncertainties in vertex position and axis orientations. The uncertainties were defined as the amount of parameter variation which results in a doubling of the RMS residuals from the minimum value 0.0053 m. The vector in **Table 9** may be multiplied by each of the previous tables to obtain the (correlated) errors in marker positions.

Table 9: Uncertainties in fitted parameters. Changing the best fit values by these amounts result in a doubling of the RMS residual fitting error.

Parameter	Error
V_x	0.0064 m
V_x	0.0073 m
V_x	0.0050 m
θ_{CM}	2.73 10^{-6} rad
θ_{DM}	2.73 10^{-6} rad
θ_z	1.93 10^{-6} rad

2.3 Hanford Local Coordinate Systems in each station

Table 10, **Table 11**, **Table 12**, **Table 13** and **Table 14** present the direction cosines between the global coordinate system and the local coordinate systems for each station. The local coordinates are defined in LIGO-L950128 and LIGO-T950004 listed in **Table 1**.

Table 10: Hanford Vertex Global-Local System Direction Cosines

	$\hat{x}_L$	$\hat{y}_L$	$\hat{z}_L$
$\hat{x}_G$	1 - 1.91886 10^{-7}	7.7333e-9	-0.00061949
$\hat{y}_G$	7.7333 10^{-9}	1 - 7.7916 10^{-11}	0.0000124832
$\hat{z}_G$	0.00061949	-0.0000124832	1 - 1.91964 10^{-7}

Table 11: Hanford X End Station (d= 4000m) Global-Local System Direction Cosines

	$\hat{x}_L$	$\hat{y}_L$	$\hat{z}_L$
$\hat{x}_G$	1 - 3.07241 10^{-11}	0	7.8389 10^{-6}
$\hat{y}_G$	0	1 - 6.6491 10^{-11}	0.0000115318
$\hat{z}_G$	-7.8389 10^{-6}	-0.0000115318	1 - 9.7215 10^{-11}

Table 12: Hanford Y End Station (d= 4000m) Global-Local System Direction Cosines

	$\hat{x}_L$	$\hat{y}_L$	$\hat{z}_L$
$\hat{x}_G$	1 - 1.92477 10^{-7}	3.9659 10^{-7}	-0.00062045
$\hat{y}_G$	3.9659 10^{-7}	1 - 2.04288 10^{-7}	0.00063920
$\hat{z}_G$	0.00062045	-0.00063920	1 - 3.9677 10^{-7}

Table 13: Hanford X Mid-Station (d = 2000m) Global-Local System Direction Cosines

	$\hat{x}_L$	$\hat{y}_L$	$\hat{z}_L$
$\hat{x}_G$	1 - 4.6765 10^{-8}	3.6722 10^{-9}	-0.000305827
$\hat{y}_G$	3.6722 10^{-9}	1 - 7.2090 10^{-11}	0.0000120075
$\hat{z}_G$	0.000305827	-0.0000120075	1 - 4.6837 10^{-8}

Table 14: Hanford Y Mid-Station (d = 2000m) Global-Local System Direction Cosines

	$\hat{x}_L$	$\hat{y}_L$	$\hat{z}_L$
$\hat{x}_G$	1 - 1.92182 10^{-7}	2.02012 10^{-7}	-0.00061997
$\hat{y}_G$	2.02012 10^{-7}	1 - 5.3086 10^{-8}	0.00032584
$\hat{z}_G$	0.00061997	-0.00032584	1 - 2.45268 10^{-7}

3 LIVINGSTON SURVEY DATA

The alignment of the Livingston beam tube arms proceeded in a different manner from what was done at Hanford. Excellent experience with the Beam Tube contractor in Hanford, combined with correspondingly negative experience with the surveying contractor in Livingston led to a decision to use the CB&I alignment database as the primary basis for determining the best estimate of the beam tube alignment. Although similar BT/VE interface markers exist for Livingston, it is believed that better accuracy could be achieved by using 64 control points measured by CB&I directly on the beam tube with GPS methods. This was possible in Livingston because CB&I bored perforations along the top of the Beam Tube Enclosure, and these allowed directly contacting survey measurements to be made of the beam tube. These data were used for the analysis reported here.

For completeness, the BTVE interface markers that were installed in Livingston are also reported. These points defined the interface positions for the beam tube (BT) and vacuum equipment (VE)

contracts. These points are identified by suitably inscribed marks on each of six brass markers, denoted {BT/VE1, BT/VE3, BT/VE4, BT/VE5, BT/VE7, BT/VE8} (see D950021 for specifications). The design positions in global coordinates of the interface markers are given in **Table 15**. ***Note that these were NOT used in the regression analysis.***

Table 15: Design values of the global coordinate positions of BT/VE interface markers

Marker ID[a]	X_G	Y_G	Z_G
BT/VE 1	46.000	0.000	-1.070[b]
BT/VE 3	2017.433	0.000	-1.070
BT/VE 4	3988.500	0.000	-1.070
BT/VE 5	0.000	46.000	-1.070
BT/VE 7	0.000	2017.433	-1.070
BT/VE 8	0.000	3988.500	-1.070

a. The same nomenclature for the BT/VE markers was used as at Hanford. Since Livingston has no mid-stations, only one marker was placed at the 2km points. Hence BT/VE 2 and BT/VE 6 do not exist.
b. The design for the BT centerline was to be 1.070 m above the finished slab.

BT/VE1 - BT/VE4 lie along the Y arm and BT/VE5 - BT/VE8 are arranged along the X arm.

During the course of constructing the beam tubes, the markers were surveyed a number of times by the Beam Tube contractor (CB&I) and by a professional surveying company (JSB). **Table 16** presents the survey results for the six BT/VE markers. The markers were placed on the as-built beam tube slabs. Their heights are affected by slight irregularities in the slab finish. After the first survey by JSB, LIGO determined the best estimate (at that time) for the vertical offsets above each of the markers where the beam tube centerline should be located. The last column in the table shows these vertical offsets.

Table 16: Cardinal Marker Survey Data for Livingston

Marker ID *Source*	*Latitude[N]*			*Longitude[W}*			*Ellipsoidal height of marker*	*Design height of beam centerline above marker elevation*
	°	′	″	°	′	″	*m*	*m*
BT/VE1								
JSB[a]	30	33	44.996494	90	46	26.740208	-7.638	1.034[b]
JSB[c]	30	33	44.996471	90	46	26.739908	-7.638	-
BT/VE3								
JSB[a]	30	32	44.013807	90	46	4.232303	-8.549	1.061[b]
JSB[c]	30	32	44.013807	90	46	4.232303	-8.549	-

Table 16: Cardinal Marker Survey Data for Livingston

Marker ID *Source*	*Latitude[N]*			*Longitude[W}*			*Ellipsoidal height of marker*	*Design height of beam centerline above marker elevation*
	°	′	″	°	′	″	*m*	*m*
BT/VE4								
JSB[a]	30	31	43.041625	90	45	41.736474	-8.825	1.066[b]
JSB[c]	30	31	43.041709	90	45	41.736110	-8.825	-
BT/VE5								
JSB[d]	30	33	45.964860	90	46	28.909760	-7.653	1.059[b]
JSB[c]	30	33	45.964752	90	46	28.909220	-7.653	-
BT/VE7								
JSB[d]	30	32	44.013807	90	46	4.232303	-7.943	1.057[b]
JSB[c]	30	33	26.478149	90	47	39.374652	-7.943	-
BT/VE8								
JSB[d]	30	33	6.984673	90	48	49.818452	-7.652	1.080[b]
JSB[c]	30	33	6.984673	90	48	49.818452	-7.652	-

a. 1 December 1997 data, JSB LIGO-C982063-00; NOTE: *BTVE3 is identical to BTVE7, implying an error in the JSB report*.
b. TDM LIGO-C972035-00 to CB&I
c. April 1998 data, JSB LIGO-C982063-00.
d. 18 December 1997 data, JSB LIGO-C982063-00; NOTE: *BTVE7 is identical to BTVE3, implying an error in the JSB report*.

Table 17 lists the 64 control points reported by CB&I as the final alignment data for the beam tube. The control points were measured directly contacting the beam tube

.

Table 17: Control Point CB&I Survey Data

CB&I Marker ID *Source*	*Latitude[N]*			*Longitude[W]*			*Ellipsoidal height of BT CL*
	°	′	″	°	′	″	*m*
X arm, Module 1							
007-L-SW-7-06	30	33	44.84322	90	46	32.96651	-6.619
013-L-SW-7-12	30	33	43.66847	90	46	37.21612	-6.657
019-L-SW-7-18	30	33	42.49373	90	46	41.46493	-6.682
025-L-SW-7-24	30	33	41.3189	90	46	45.71427	-6.712
031-L-SW-7-30	30	33	40.14409	90	46	49.96287	-6.741
037-L-SW-7-36	30	33	38.96912	90	46	54.21174	-6.764
043-L-SW-7-42	30	33	37.79447	90	46	58.46065	-6.787
049-L-SW-7-48	30	33	36.61928	90	47	2.70953	-6.805
055-L-SW-7-54	30	33	35.44441	90	47	6.9584	-6.824
061-L-SW-7-60	30	33	34.26942	90	47	11.20717	-6.839
067-L-SW-7-66	30	33	33.09422	90	47	15.45617	-6.85
073-L-SW-7-72	30	33	31.91912	90	47	19.70463	-6.864
079-L-SW-7-78	30	33	30.7442	90	47	23.95327	-6.873
085-L-SW-7-84	30	33	29.56901	90	47	28.20187	-6.879
091-L-SW-7-90	30	33	28.39329	90	47	32.45168	-6.881
095-L-SW-7-94	30	33	27.60975	90	47	35.28413	-6.884
X arm, Module 2							
007-L-SW-8-06	30	33	25.35021	90	47	43.45273	-6.884
011-L-SW-8-10	30	33	24.56673	90	47	46.28478	-6.880
017-L-SW-8-16	30	33	23.39107	90	47	50.53357	-6.871
023-L-SW-8-22	30	33	22.21583	90	47	54.78214	-6.867
029-L-SW-8-28	30	33	21.04034	90	47	59.03045	-6.853
035-L-SW-8-34	30	33	19.86488	90	48	3.27876	-6.849
041-L-SW-8-40	30	33	18.68923	90	48	7.52733	-6.834
047-L-SW-8-46	30	33	17.51372	90	48	11.77571	-6.819
053-L-SW-8-52	30	33	16.33795	90	48	16.02414	-6.797
059-L-SW-8-58	30	33	15.1623	90	48	20.27255	-6.778
065-L-SW-8-64	30	33	13.98671	90	48	24.52062	-6.755
071-L-SW-8-70	30	33	12.81112	90	48	28.76863	-6.726
077-L-SW-8-76	30	33	11.63519	90	48	33.01682	-6.701
083-L-SW-8-82	30	33	10.45933	90	48	37.26522	-6.67
089-L-SW-8-88	30	33	9.28357	90	48	41.51372	-6.638
095-L-SW-8-94	30	33	8.10749	90	48	45.76245	-6.609

Table 17: Control Point CB&I Survey Data

CB&I Marker ID *Source*	*Latitude[N]*			*Longitude[W]*			*Ellipsoidal height of BT CL*
	°	′	″	°	′	″	*m*
Y arm, Module1							
-L-SE-5-06	30	33	41.51672	90	46	25.45574	-6.666
013-L-SE-5-12	30	33	37.80886	90	46	24.08704	-6.741
019-L-SE-5-18	30	33	34.13159	90	46	22.72963	-6.805
025-L-SE-5-24	30	33	30.45399	90	46	21.37209	-6.869
031-L-SE-5-30	30	33	26.77698	90	46	20.01464	-6.931
037-L-SE-5-36	30	33	23.09977	90	46	18.65745	-6.985
043-L-SE-5-42	30	33	19.42326	90	46	17.30056	-7.045
049-L-SE-5-48	30	33	15.74548	90	46	15.94307	-7.102
055-L-SE-5-54	30	33	12.06884	90	46	14.58607	-7.158
061-L-SE-5-60	30	33	8.39187	90	46	13.22903	-7.205
067-L-SE-5-66	30	33	4.71473	90	46	11.87175	-7.256
073-L-SE-5-72	30	33	1.03757	90	46	10.51468	-7.296
079-L-SE-5-78	30	32	57.36069	90	46	9.15775	-7.345
085-L-SE-5-84	30	32	53.68373	90	46	7.80083	-7.387
091-L-SE-5-90	30	32	50.0063	90	46	6.44356	-7.426
095-L-SE-5-94	30	32	47.55538	90	46	5.53913	-7.451
Y arm, Module 2							
007-L-SE-6-06	30	32	40.48398	90	46	2.92976	-7.518
011-L-SE-6-10	30	32	38.03278	90	46	2.02525	-7.54
017-L-SE-6-16	30	32	34.35561	90	46	0.66832	-7.57
023-L-SE-6-22	30	32	30.67897	90	45	59.31167	-7.592
029-L-SE-6-28	30	32	27.00148	90	45	57.9548	-7.624
035-L-SE-6-34	30	32	23.32402	90	45	56.59774	-7.647
041-L-SE-6-40	30	32	19.64763	90	45	55.24134	-7.671
047-L-SE-6-46	30	32	15.96996	90	45	53.88442	-7.687
053-L-SE-6-52	30	32	12.29286	90	45	52.5279	-7.703
059-L-SE-6-58	30	32	8.61604	90	45	51.17127	-7.716
065-L-SE-6-64	30	32	4.9388	90	45	49.81468	-7.728
071-L-SE-6-70	30	32	1.26155	90	45	48.45788	-7.739
077-L-SE-6-76	30	31	57.58426	90	45	47.10137	-7.746
083-L-SE-6-82	30	31	53.90631	90	45	45.74429	-7.753
089-L-SE-6-88	30	31	50.22968	90	45	44.388	-7.759
095-L-SE-6-94	30	31	46.55246	90	45	43.03153	-7.755

The global coordinate axes were determined by fitting two orthogonal axes going through the data.

3.1 Fit to the Survey Data

Refer to **Section 2.1** for the details of the fitting procedure. Briefly, the data of **Table 17** were converted to the earth-fixed Cartesian system, $\{\hat{x}_E, \hat{y}_E, \hat{z}_E\}$. The earth model WGS-84 was used for transformation. The set of orthonormal axes which best describes the Courtesan data for the mark-

ers were determined by a χ^2 minimization of the transverse (2D) residuals of the control points. There are six degrees of freedom for the fit: 3 translational and three rotational. These were chosen as:

- **three** coordinates for the vertex, $\{X_v, Y_v, Z_v\}$;
- **two** direction cosines for one axis, $\{n_{xx}, n_{xy}, 1\}$; the z component was fixed.
- **one** direction cosine for the remaining axis (the orientation of the remaining axis in the plane normal to the first axis), $\left\{n_{yx}, \frac{-(n_{xx}n_{yx}+1)}{n_{xy}}, 1\right\}$; this is done by fitting the x component of the second normal, constraining the y and z components.

The errors associated with the measured data were not reported in the survey; however experience has shown that the general accuracy CB&I was able to achieve using GPS is typically 0.005 m RMS (3-axis). The fitting procedure assumed equal weights for all data: the χ^2 optimization was reduced to a least squares minimization.

In fact, the 3-axis RMS residual for the best fit was 0.0040 m. This fit gives parameter values listed in **Table 18**.

Table 18: Parameters resulting from best fit to the survey data for Livingston, LA

Parameter	*Value*	*Estimated Error*	*Units*
Vertex	Global $\{\hat{x}_G, \hat{y}_G, \hat{z}_G\}$: {0,0,0}	{.0062, .0055, .0041}	m
	Geodetic $\{h, \phi, \lambda\}$:{-6.574, {30,33,46.4196}, {-90,46,27.2654}}	-	{m, deg, deg}
	Earth-fixed $\{\hat{x}_E, \hat{y}_E, \hat{z}_E\}$: {-74276.044, -5.496283721 10^6, 3.224257018 10^6}	{.0062, .0055, .0041}	m
$\hat{x}_G$	Global $\{\hat{x}_G, \hat{y}_G, \hat{z}_G\}$: {1,0,0}	-	
	Earth-fixed $\{\hat{x}_E, \hat{y}_E, \hat{z}_E\}$: {-0.954574, -0.14158, -0.262189}	-	
	Compass Direction: S72.2835° W (ref. geodetic north)[a]	1.73 10^{-6}	radian
	Angle *below* local horizontal at Vertex: 3.121 10^{-4}	2.44 10^{-6}	radian
$\hat{y}_G$	Global $\{\hat{x}_G, \hat{y}_G, \hat{z}_G\}$: {0,1,0}	-	
	Earth-fixed $\{\hat{x}_E, \hat{y}_E, \hat{z}_E\}$: {0.297741,-0.48791,-0.820545}	-	
	Compass Direction: S17.7165° E (see footnote a)	1.73 10^{-6}	radian
	Angle *below* local horizontal at Vertex: 6.107 10^{-4}	2.44 10^{-6}	radian

Table 18: Parameters resulting from best fit to the survey data for Livingston, LA

Parameter	*Value*	*Estimated Error*	*Units*
$\hat{z}_G$	Global $\{\hat{x}_G, \hat{y}_G, \hat{z}_G\}$: {0,0,1}	-	
	Earth-fixed $\{\hat{x}_E, \hat{y}_E, \hat{z}_E\}$: {-0.0117515,-0.861335,0.507901}	-	
	Deviation from zenith at vertex, *toward* $\hat{x}_G$: $3.121\ 10^{-4}$ *toward* $\hat{y}_G$: $6.107\ 10^{-4}$	$2.44\ 10^{-6}$	radian

a. Site drawings call for arms to run S72° W and S18° E; these are referred to the LA state plane coordinates (northing & easting). Geodetic north is 17' 1" (~ 0.28°) W of grid north at the vertex.

Location of as-built BT/VE markers relative to global coordinate system

Using the coordinate system described above, the positions for each of the 6 BT/VE interface markers were determined by averaging the residuals from multiple measurements of individual markers. **Table 19** presents the results.

Table 19: Global coordinate positions of as-built BT/VE interface markers

Marker ID	X_G	Y_G	Z_G
BT/VE 1	**TBD**	**TBD**	**TBD**
BT/VE 2	**TBD**	**TBD**	**TBD**
BT/VE 4	**TBD**	**TBD**	**TBD**
BT/VE 5	**TBD**	**TBD**	**TBD**
BT/VE 6	**TBD**	**TBD**	**TBD**
BT/VE 8	**TBD**	**TBD**	**TBD**

The positions of the 64 CB&I control points relative to the global coordinate system are listed in **Table 20**.

Table 20: Global coordinate positions of CB&I control points, meters

CB&I Marker ID	X_G	Y_G	Z_G
X arm			
007-L-SW-7-06	159.498	0.007	0.002
013-L-SW-7-12	278.385	0.003	-0.003
019-L-SW-7-18	397.252	0.004	0.003
025-L-SW-7-24	516.133	0.001	0.001
031-L-SW-7-30	634.996	0.003	-0.001
037-L-SW-7-36	753.868	0.006	0.000
043-L-SW-7-42	872.738	-0.002	-0.001
049-L-SW-7-48	991.613	0.004	0.001
055-L-SW-7-54	1110.485	0.000	-0.001
061-L-SW-7-60	1229.356	-0.001	-0.001
067-L-SW-7-66	1348.235	0.001	0.002
073-L-SW-7-72	1467.100	0.002	-0.002
079-L-SW-7-78	1585.967	-0.004	-0.002
085-L-SW-7-84	1704.837	-0.003	-0.001
091-L-SW-7-90	1823.743	0.002	0.001
095-L-SW-7-94	1902.992	0.002	-0.001
007-L-SW-8-06	2131.541	-0.003	-0.002
011-L-SW-8-10	2210.78	-0.003	0.000
017-L-SW-8-16	2329.661	0.002	0.004
023-L-SW-8-22	2448.533	-0.004	0.001
029-L-SW-8-28	2567.400	-0.002	0.005
035-L-SW-8-34	2686.268	-0.002	-0.003
041-L-SW-8-40	2805.145	-0.001	-0.002
047-L-SW-8-46	2924.016	-0.003	-0.003
053-L-SW-8-52	3042.891	0.001	0.000
059-L-SW-8-58	3161.765	0.000	-0.001
065-L-SW-8-64	3280.603	-0.002	-0.001
071-L-SW-8-70	3399.494	-0.004	0.003
077-L-SW-8-76	3518.365	0.001	0.000
083-L-SW-8-82	3637.242	0.001	0.002
089-L-SW-8-88	3756.121	-0.005	0.002
095-L-SW-8-94	3875.009	-0.004	-0.003

Table 20: Global coordinate positions of CB&I control points, meters

CB&I Marker ID	X_G	Y_G	Z_G
Y arm			
-L-SE-5-06	0.006	158.498	0.002
013-L-SE-5-12	0.007	278.366	-0.004
019-L-SE-5-18	0.007	397.245	-0.002
025-L-SE-5-24	0.005	516.135	-0.002
031-L-SE-5-30	0.000	635.007	-0.002
037-L-SE-5-36	0.003	753.883	0.004
043-L-SE-5-42	0.005	872.736	0.001
049-L-SE-5-48	0.004	991.631	-0.001
055-L-SE-5-54	0.004	1110.489	-0.004
061-L-SE-5-60	0.005	1229.357	0.000
067-L-SE-5-66	0.000	1348.232	-0.003
073-L-SE-5-72	0.001	1467.106	0.004
079-L-SE-5-78	0.001	1585.970	-0.001
085-L-SE-5-84	0.002	1704.837	-0.001
091-L-SE-5-90	-0.002	1823.721	-0.001
095-L-SE-5-94	-0.002	1902.953	-0.001
007-L-SE-6-06	0.001	2131.553	-0.001
011-L-SE-6-10	0.001	2210.794	-0.001
017-L-SE-6-16	-0.001	2329.668	-0.001
023-L-SE-6-22	-0.001	2448.524	0.005
029-L-SE-6-28	0.001	2567.407	-0.002
035-L-SE-6-34	-0.003	2686.290	-0.001
041-L-SE-6-40	-0.002	2805.137	-0.004
047-L-SE-6-46	-0.002	2924.026	-0.001
053-L-SE-6-52	0.002	3042.895	0.000
059-L-SE-6-58	-0.001	3161.757	0.001
065-L-SE-6-64	0.001	3280.631	0.002
071-L-SE-6-70	-0.003	3399.507	0.001
077-L-SE-6-76	-0.001	3518.382	0.002
083-L-SE-6-82	-0.007	3637.281	0.000
089-L-SE-6-88	-0.006	3756.135	-0.002
095-L-SE-6-94	-0.006	3875.00	0.003

The scatter of the residuals is presented graphically in **Figure 5** and **Figure 6**. **Figure 5** presents the scatter in the plane normal to the axis for each arm. There is an apparent greater right-left scatter along the X arm. This is a result means that the best description of the beam tube centerline positions corresponds to two axes which are not exactly orthogonal: an optimization without imposing the orthogonality constraint between the best fit lines results in axes having an included angle ~ 6.1 microradians greater than 90 degrees. This fact may be seen in the lower panels of **Figure 6** which present residuals in the horizontal and vertical plane as a function of their position along the arms.

Figure 5: Scatter plots of fit residuals in plane normal to global axis for Livingston, LA.

X Arm

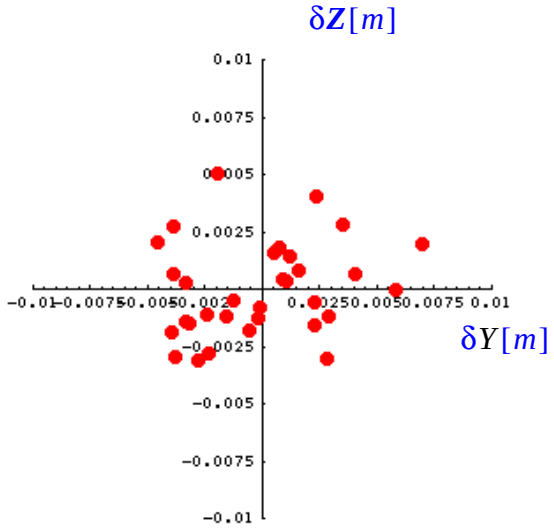

Y Arm

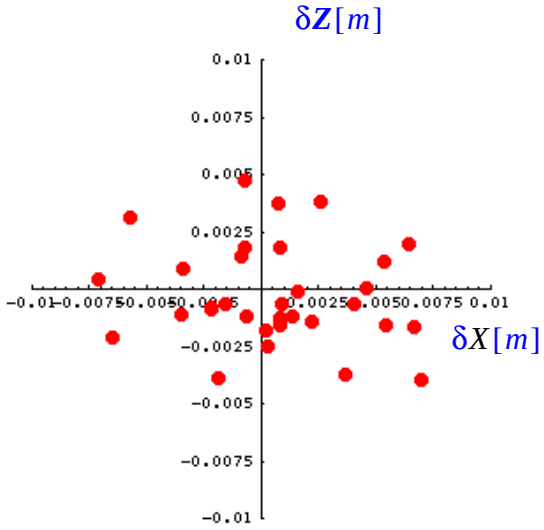

Figure 6: Dependence of residuals on distance along the arms for Livingston, LA.

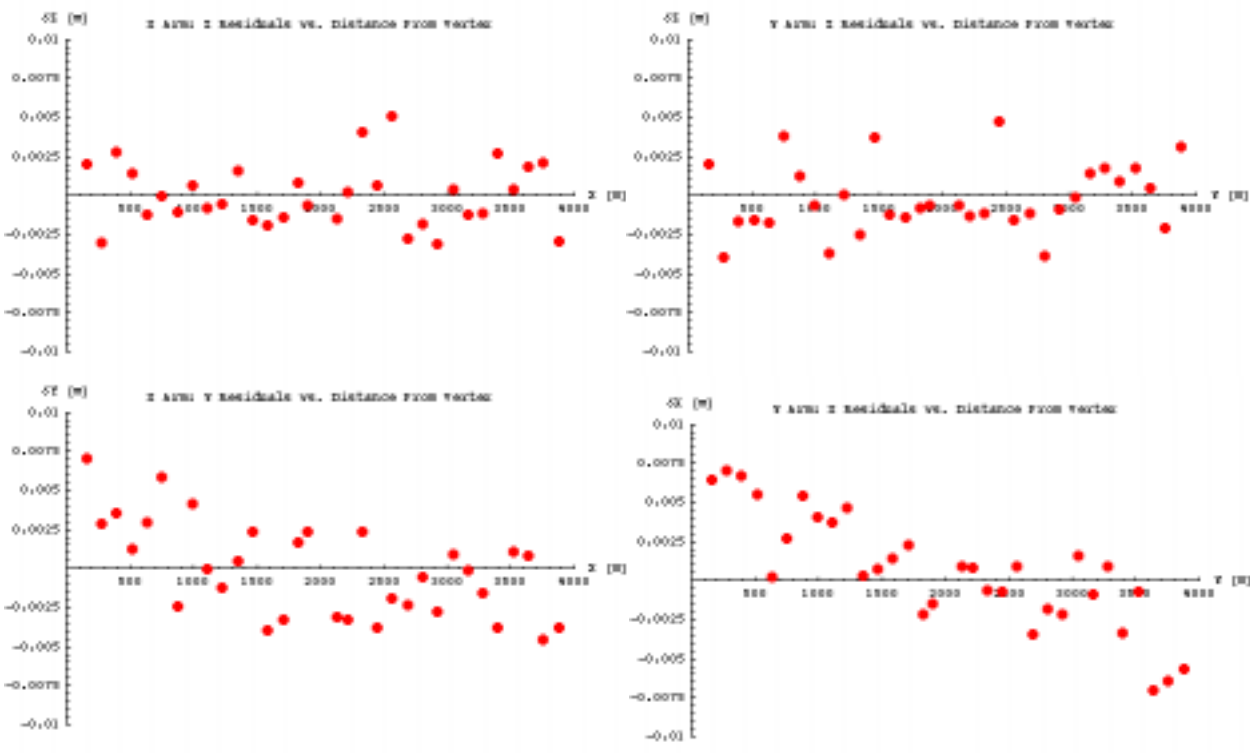

3.2 Error propagators in the fits

Any error in the estimated position of the vertex results in a common mode offset to all marker positions; errors in the estimated directions of the coordinate axis result in either differential mode or common mode offsets according which orientation angle is in error and the effect on marker position is in proportion to marker distances from the vertex. This behavior is represented by the error propagation matrices presented as **Table 21**, **Table 22** and **Table 23**. Each table corresponds to one coordinate. The rows give the effects of parameter variations the eight marker locations. Vertex translational errors are referred along the global axes. Angular errors in the orientation of the axes are referred to roll, pitch and yaw of the $\hat{z}_G$ axis. Refer to **Figure 4** in **Section 2.2** for definitions.

Table 21: Sensitivity matrix for the X_G coordinate for control points

CB&I Marker ID	$\frac{\partial}{\partial V_x}$ [m/m]	$\frac{\partial}{\partial V_y}$ [m/m]	$\frac{\partial}{\partial V_z}$ [m/m]	$\frac{\partial}{\partial \theta_{CM}}$ [m/rad]	$\frac{\partial}{\partial \theta_{DM}}$ [m/rad]	$\frac{\partial}{\partial \theta_z}$ [m/rad]
X arm						
007-L-SW-7-06	-0.955	-0.142	-0.262	-0.001	-0.001	0.007
013-L-SW-7-12	-0.955	-0.142	-0.262	0.002	0.002	0.003
019-L-SW-7-18	-0.955	-0.142	-0.262	-0.002	-0.002	0.004
025-L-SW-7-24	-0.955	-0.142	-0.262	-0.001	-0.001	0.001
031-L-SW-7-30	-0.955	-0.142	-0.262	0.001	0.001	0.003
037-L-SW-7-36	-0.955	-0.142	-0.262	0.000	0.000	0.006
043-L-SW-7-42	-0.955	-0.142	-0.262	0.001	0.001	-0.002
049-L-SW-7-48	-0.955	-0.142	-0.262	0.000	0.000	0.004
055-L-SW-7-54	-0.955	-0.142	-0.262	0.001	0.001	0.000
061-L-SW-7-60	-0.955	-0.142	-0.262	0.000	0.000	-0.001
067-L-SW-7-66	-0.955	-0.142	-0.262	-0.001	-0.001	0.001
073-L-SW-7-72	-0.955	-0.142	-0.262	0.001	0.001	0.002
079-L-SW-7-78	-0.955	-0.142	-0.262	0.001	0.001	-0.004
085-L-SW-7-84	-0.955	-0.142	-0.262	0.001	0.001	-0.003
091-L-SW-7-90	-0.955	-0.142	-0.262	-0.001	-0.001	0.002
095-L-SW-7-94	-0.955	-0.142	-0.262	0.000	0.000	0.002
007-L-SW-8-06	-0.955	-0.142	-0.262	0.001	0.001	-0.003
011-L-SW-8-10	-0.955	-0.142	-0.262	0.000	0.000	-0.003
017-L-SW-8-16	-0.955	-0.142	-0.262	-0.003	-0.003	0.002
023-L-SW-8-22	-0.955	-0.142	-0.262	0.000	0.000	-0.004
029-L-SW-8-28	-0.955	-0.142	-0.262	-0.004	-0.004	-0.002
035-L-SW-8-34	-0.955	-0.142	-0.262	0.002	0.002	-0.002
041-L-SW-8-40	-0.955	-0.142	-0.262	0.001	0.001	-0.001
047-L-SW-8-46	-0.955	-0.142	-0.262	0.002	0.002	-0.003
053-L-SW-8-52	-0.955	-0.142	-0.262	0.000	0.000	0.001
059-L-SW-8-58	-0.955	-0.142	-0.262	0.001	0.001	0.000
065-L-SW-8-64	-0.955	-0.142	-0.262	0.001	0.001	-0.002
071-L-SW-8-70	-0.955	-0.142	-0.262	-0.002	-0.002	-0.004
077-L-SW-8-76	-0.955	-0.142	-0.262	0.000	0.000	0.001
083-L-SW-8-82	-0.955	-0.142	-0.262	-0.001	-0.001	0.001
089-L-SW-8-88	-0.955	-0.142	-0.262	-0.001	-0.001	-0.005
095-L-SW-8-94	-0.955	-0.142	-0.262	0.002	0.002	-0.000

Table 21: Sensitivity matrix for the X_G coordinate for control points

CB&I Marker ID	$\frac{\partial}{\partial V_x}$ [m/m]	$\frac{\partial}{\partial V_y}$ [m/m]	$\frac{\partial}{\partial V_z}$ [m/m]	$\frac{\partial}{\partial \theta_{CM}}$ [m/rad]	$\frac{\partial}{\partial \theta_{DM}}$ [m/rad]	$\frac{\partial}{\partial \theta_z}$ [m/rad]
Y arm						
-L-SE-5-06	-0.955	-0.142	-0.262	-0.001	-0.001	158.498
013-L-SE-5-12	-0.955	-0.142	-0.262	0.003	0.003	278.366
019-L-SE-5-18	-0.955	-0.142	-0.262	0.001	0.001	397.245
025-L-SE-5-24	-0.955	-0.142	-0.262	0.001	0.001	516.135
031-L-SE-5-30	-0.955	-0.142	-0.262	0.001	0.001	635.007
037-L-SE-5-36	-0.955	-0.142	-0.262	-0.003	-0.003	753.883
043-L-SE-5-42	-0.955	-0.142	-0.262	-0.001	-0.001	872.736
049-L-SE-5-48	-0.955	-0.142	-0.262	0.000	0.000	991.631
055-L-SE-5-54	-0.955	-0.142	-0.262	0.003	0.003	1110.489
061-L-SE-5-60	-0.955	-0.142	-0.262	0.000	0.000	1229.357
067-L-SE-5-66	-0.955	-0.142	-0.262	0.002	0.002	1348.232
073-L-SE-5-72	-0.955	-0.142	-0.262	-0.003	-0.003	1467.106
079-L-SE-5-78	-0.955	-0.142	-0.262	0.001	0.001	1585.97
085-L-SE-5-84	-0.955	-0.142	-0.262	0.001	0.001	1704.837
091-L-SE-5-90	-0.955	-0.142	-0.262	0.001	0.001	1823.721
095-L-SE-5-94	-0.955	-0.142	-0.262	0.000	0.000	1902.953
007-L-SE-6-06	-0.955	-0.142	-0.262	0.000	0.000	2131.553
011-L-SE-6-10	-0.955	-0.142	-0.262	0.001	0.001	2210.794
017-L-SE-6-16	-0.955	-0.142	-0.262	0.001	0.001	2329.668
023-L-SE-6-22	-0.955	-0.142	-0.262	-0.003	-0.003	2448.524
029-L-SE-6-28	-0.955	-0.142	-0.262	0.001	0.001	2567.407
035-L-SE-6-34	-0.955	-0.142	-0.262	0.001	0.001	2686.29
041-L-SE-6-40	-0.955	-0.142	-0.262	0.003	0.003	2805.137
047-L-SE-6-46	-0.955	-0.142	-0.262	0.001	0.001	2924.026
053-L-SE-6-52	-0.955	-0.142	-0.262	0.000	0.000	3042.895
059-L-SE-6-58	-0.955	-0.142	-0.262	-0.001	-0.001	3161.757
065-L-SE-6-64	-0.955	-0.142	-0.262	-0.001	-0.001	3280.631
071-L-SE-6-70	-0.955	-0.142	-0.262	-0.001	-0.001	3399.507
077-L-SE-6-76	-0.955	-0.142	-0.262	-0.001	-0.001	3518.382
083-L-SE-6-82	-0.955	-0.142	-0.262	0.000	0.000	3637.281
089-L-SE-6-88	-0.955	-0.142	-0.262	0.001	0.001	3756.135
095-L-SE-6-94	-0.955	-0.142	-0.262	-0.002	-0.002	3875.008

Table 22: Sensitivity matrix for the Y_G coordinate for control points

CB&I Marker ID	$\frac{\partial}{\partial V_x}$ [m/m]	$\frac{\partial}{\partial V_y}$ [m/m]	$\frac{\partial}{\partial V_z}$ [m/m]	$\frac{\partial}{\partial \theta_{CM}}$ [m/rad]	$\frac{\partial}{\partial \theta_{DM}}$ [m/rad]	$\frac{\partial}{\partial \theta_z}$ [m/rad]
X arm						
007-L-SW-7-06	0.298	-0.488	-0.821	-0.001	0.001	-159.498
013-L-SW-7-12	0.298	-0.488	-0.821	0.002	-0.002	-278.385
019-L-SW-7-18	0.298	-0.488	-0.821	-0.002	0.002	-397.252
025-L-SW-7-24	0.298	-0.488	-0.821	-0.001	0.001	-516.133
031-L-SW-7-30	0.298	-0.488	-0.821	0.001	-0.001	-634.996
037-L-SW-7-36	0.298	-0.488	-0.821	0.000	0.000	-753.868
043-L-SW-7-42	0.298	-0.488	-0.821	0.001	-0.001	-872.738
049-L-SW-7-48	0.298	-0.488	-0.821	0.000	0.000	-991.613
055-L-SW-7-54	0.298	-0.488	-0.821	0.001	-0.001	-1110.485
061-L-SW-7-60	0.298	-0.488	-0.821	0.000	0.000	-1229.356
067-L-SW-7-66	0.298	-0.488	-0.821	-0.001	0.001	-1348.235
073-L-SW-7-72	0.298	-0.488	-0.821	0.001	-0.001	-1467.1
079-L-SW-7-78	0.298	-0.488	-0.821	0.001	-0.001	-1585.967
085-L-SW-7-84	0.298	-0.488	-0.821	0.001	-0.001	-1704.837
091-L-SW-7-90	0.298	-0.488	-0.821	-0.001	0.001	-1823.743
095-L-SW-7-94	0.298	-0.488	-0.821	0.000	0.000	-1902.992
007-L-SW-8-06	0.298	-0.488	-0.821	0.001	-0.001	-2131.541
011-L-SW-8-10	0.298	-0.488	-0.821	0.000	0.000	-2210.78
017-L-SW-8-16	0.298	-0.488	-0.821	-0.003	0.003	-2329.661
023-L-SW-8-22	0.298	-0.488	-0.821	0.000	0.000	-2448.533
029-L-SW-8-28	0.298	-0.488	-0.821	-0.004	0.004	-2567.4
035-L-SW-8-34	0.298	-0.488	-0.821	0.002	-0.002	-2686.268
041-L-SW-8-40	0.298	-0.488	-0.821	0.001	-0.001	-2805.145
047-L-SW-8-46	0.298	-0.488	-0.821	0.002	-0.002	-2924.016
053-L-SW-8-52	0.298	-0.488	-0.821	0.000	0.000	-3042.891
059-L-SW-8-58	0.298	-0.488	-0.821	0.001	-0.001	-3161.765
065-L-SW-8-64	0.298	-0.488	-0.821	0.001	-0.001	-3280.63
071-L-SW-8-70	0.298	-0.488	-0.821	-0.002	0.002	-3399.494
077-L-SW-8-76	0.298	-0.488	-0.821	0.000	0.000	-3518.365
083-L-SW-8-82	0.298	-0.488	-0.821	-0.001	0.001	-3637.242
089-L-SW-8-88	0.298	-0.488	-0.821	-0.001	0.001	-3756.121
095-L-SW-8-94	0.298	-0.488	-0.821	0.002	-0.002	-3875.009

Table 22: Sensitivity matrix for the Y_G coordinate for control points

CB&I Marker ID	$\frac{\partial}{\partial V_x}$ [m/m]	$\frac{\partial}{\partial V_y}$ [m/m]	$\frac{\partial}{\partial V_z}$ [m/m]	$\frac{\partial}{\partial \theta_{CM}}$ [m/rad]	$\frac{\partial}{\partial \theta_{DM}}$ [m/rad]	$\frac{\partial}{\partial \theta_z}$ [m/rad]
Y arm						
-L-SE-5-06	0.298	-0.488	-0.821	-0.001	0.001	-0.006
013-L-SE-5-12	0.298	-0.488	-0.821	0.003	-0.003	-0.007
019-L-SE-5-18	0.298	-0.488	-0.821	0.001	-0.001	-0.007
025-L-SE-5-24	0.298	-0.488	-0.821	0.001	-0.001	-0.005
031-L-SE-5-30	0.298	-0.488	-0.821	0.001	-0.001	0.000
037-L-SE-5-36	0.298	-0.488	-0.821	-0.003	0.003	-0.003
043-L-SE-5-42	0.298	-0.488	-0.821	-0.001	0.001	-0.005
049-L-SE-5-48	0.298	-0.488	-0.821	0.000	0.000	-0.004
055-L-SE-5-54	0.298	-0.488	-0.821	0.003	-0.003	-0.004
061-L-SE-5-60	0.298	-0.488	-0.821	0.000	0.000	-0.005
067-L-SE-5-66	0.298	-0.488	-0.821	0.002	-0.002	0.000
073-L-SE-5-72	0.298	-0.488	-0.821	-0.003	0.003	-0.001
079-L-SE-5-78	0.298	-0.488	-0.821	0.001	-0.001	-0.001
085-L-SE-5-84	0.298	-0.488	-0.821	0.001	-0.001	-0.002
091-L-SE-5-90	0.298	-0.488	-0.821	0.001	-0.001	0.002
095-L-SE-5-94	0.298	-0.488	-0.821	0.000	0.000	0.002
007-L-SE-6-06	0.298	-0.488	-0.821	0.000	0.000	-0.001
011-L-SE-6-10	0.298	-0.488	-0.821	0.001	-0.001	-0.001
017-L-SE-6-16	0.298	-0.488	-0.821	0.001	-0.001	0.001
023-L-SE-6-22	0.298	-0.488	-0.821	-0.003	0.003	0.001
029-L-SE-6-28	0.298	-0.488	-0.821	0.001	-0.001	-0.001
035-L-SE-6-34	0.298	-0.488	-0.821	0.001	-0.001	0.003
041-L-SE-6-40	0.298	-0.488	-0.821	0.003	-0.003	0.002
047-L-SE-6-46	0.298	-0.488	-0.821	0.001	-0.001	0.002
053-L-SE-6-52	0.298	-0.488	-0.821	0.000	0.000	-0.002
059-L-SE-6-58	0.298	-0.488	-0.821	-0.001	0.001	0.001
065-L-SE-6-64	0.298	-0.488	-0.821	-0.001	0.001	-0.001
071-L-SE-6-70	0.298	-0.488	-0.821	-0.001	0.001	0.003
077-L-SE-6-76	0.298	-0.488	-0.821	-0.001	0.001	0.001
083-L-SE-6-82	0.298	-0.488	-0.821	0.000	0.000	0.007
089-L-SE-6-88	0.298	-0.488	-0.821	0.001	-0.001	0.006
095-L-SE-6-94	0.298	-0.488	-0.821	-0.002	0.002	0.006

Table 23: Sensitivity matrix for the Z_G coordinate for control points

CB&I Marker ID	$\frac{\partial}{\partial V_x}$ [m/m]	$\frac{\partial}{\partial V_y}$ [m/m]	$\frac{\partial}{\partial V_z}$ [m/m]	$\frac{\partial}{\partial \theta_{CM}}$ [m/rad]	$\frac{\partial}{\partial \theta_{DM}}$ [m/rad]	$\frac{\partial}{\partial \theta_z}$ [m/rad]
X arm						
007-L-SW-7-06	-0.012	-0.861	0.508	112.787	112.777	0
013-L-SW-7-12	-0.012	-0.861	0.508	196.85	196.846	0
019-L-SW-7-18	-0.012	-0.861	0.508	280.902	280.897	0
025-L-SW-7-24	-0.012	-0.861	0.508	364.962	364.96	0
031-L-SW-7-30	-0.012	-0.861	0.508	449.012	449.008	0
037-L-SW-7-36	-0.012	-0.861	0.508	533.069	533.061	0
043-L-SW-7-42	-0.012	-0.861	0.508	617.117	617.121	0
049-L-SW-7-48	-0.012	-0.861	0.508	701.179	701.173	0
055-L-SW-7-54	-0.012	-0.861	0.508	785.231	785.231	0
061-L-SW-7-60	-0.012	-0.861	0.508	869.285	869.287	0
067-L-SW-7-66	-0.012	-0.861	0.508	953.346	953.346	0
073-L-SW-7-72	-0.012	-0.861	0.508	1037.398	1037.394	0
079-L-SW-7-78	-0.012	-0.861	0.508	1121.446	1121.451	0
085-L-SW-7-84	-0.012	-0.861	0.508	1205.5	1205.504	0
091-L-SW-7-90	-0.012	-0.861	0.508	1289.582	1289.58	0
095-L-SW-7-94	-0.012	-0.861	0.508	1345.62	1345.617	0
007-L-SW-8-06	-0.012	-0.861	0.508	1507.225	1507.229	0
011-L-SW-8-10	-0.012	-0.861	0.508	1563.255	1563.26	0
017-L-SW-8-16	-0.012	-0.861	0.508	1647.321	1647.317	0
023-L-SW-8-22	-0.012	-0.861	0.508	1731.371	1731.377	0
029-L-SW-8-28	-0.012	-0.861	0.508	1815.425	1815.428	0
035-L-SW-8-34	-0.012	-0.861	0.508	1899.477	1899.48	0
041-L-SW-8-40	-0.012	-0.861	0.508	1983.537	1983.538	0
047-L-SW-8-46	-0.012	-0.861	0.508	2067.59	2067.594	0
053-L-SW-8-52	-0.012	-0.861	0.508	2151.65	2151.648	0
059-L-SW-8-58	-0.012	-0.861	0.508	2235.705	2235.705	0
065-L-SW-8-64	-0.012	-0.861	0.508	2319.754	2319.757	0
071-L-SW-8-70	-0.012	-0.861	0.508	2403.802	2403.808	0
077-L-SW-8-76	-0.012	-0.861	0.508	2487.861	2487.859	0
083-L-SW-8-82	-0.012	-0.861	0.508	2571.919	2571.918	0
089-L-SW-8-88	-0.012	-0.861	0.508	2655.976	2655.982	0
095-L-SW-8-94	-0.012	-0.861	0.508	2740.043	2740.048	0

Table 23: Sensitivity matrix for the Z_G coordinate for control points

CB&I Marker ID	$\frac{\partial}{\partial V_x}$ [m/m]	$\frac{\partial}{\partial V_y}$ [m/m]	$\frac{\partial}{\partial V_z}$ [m/m]	$\frac{\partial}{\partial \theta_{CM}}$ [m/rad]	$\frac{\partial}{\partial \theta_{DM}}$ [m/rad]	$\frac{\partial}{\partial \theta_z}$ [m/rad]
Y arm						
-L-SE-5-06	-0.012	-0.861	0.508	112.08	-112.071	0
013-L-SE-5-12	-0.012	-0.861	0.508	196.84	-196.83	0
019-L-SE-5-18	-0.012	-0.861	0.508	280.9	-280.89	0
025-L-SE-5-24	-0.012	-0.861	0.508	364.967	-364.959	0
031-L-SE-5-30	-0.012	-0.861	0.508	449.018	-449.018	0
037-L-SE-5-36	-0.012	-0.861	0.508	533.078	-533.074	0
043-L-SE-5-42	-0.012	-0.861	0.508	617.121	-617.114	0
049-L-SE-5-48	-0.012	-0.861	0.508	701.192	-701.186	0
055-L-SE-5-54	-0.012	-0.861	0.508	785.237	-785.232	0
061-L-SE-5-60	-0.012	-0.861	0.508	869.29	-869.283	0
067-L-SE-5-66	-0.012	-0.861	0.508	953.344	-953.344	0
073-L-SE-5-72	-0.012	-0.861	0.508	1037.401	-1037.4	0
079-L-SE-5-78	-0.012	-0.861	0.508	1121.451	-1121.449	0
085-L-SE-5-84	-0.012	-0.861	0.508	1205.504	-1205.5	0
091-L-SE-5-90	-0.012	-0.861	0.508	1289.564	-1289.567	0
095-L-SE-5-94	-0.012	-0.861	0.508	1345.59	-1345.592	0
007-L-SE-6-06	-0.012	-0.861	0.508	1507.236	-1507.235	0
011-L-SE-6-10	-0.012	-0.861	0.508	1563.268	-1563.267	0
017-L-SE-6-16	-0.012	-0.861	0.508	1647.323	-1647.324	0
023-L-SE-6-22	-0.012	-0.861	0.508	1731.367	-1731.368	0
029-L-SE-6-28	-0.012	-0.861	0.508	1815.431	-1815.43	0
035-L-SE-6-34	-0.012	-0.861	0.508	1899.492	-1899.497	0
041-L-SE-6-40	-0.012	-0.861	0.508	1983.53	-1983.533	0
047-L-SE-6-46	-0.012	-0.861	0.508	2067.597	-2067.6	0
053-L-SE-6-52	-0.012	-0.861	0.508	2151.653	-2151.651	0
059-L-SE-6-58	-0.012	-0.861	0.508	2235.699	-2235.7	0
065-L-SE-6-64	-0.012	-0.861	0.508	2319.757	-2319.756	0
071-L-SE-6-70	-0.012	-0.861	0.508	2403.812	-2403.817	0
077-L-SE-6-76	-0.012	-0.861	0.508	2487.871	-2487.872	0
083-L-SE-6-82	-0.012	-0.861	0.508	2571.941	-2571.951	0
089-L-SE-6-88	-0.012	-0.861	0.508	2655.984	-2655.993	0
095-L-SE-6-94	-0.012	-0.861	0.508	2740.040	-2740.048	0

Table 24 presents uncertainties in vertex position and axis orientations. The uncertainties were defined as the amount of parameter variation which results in a doubling of the RMS residuals from the minimum value 0.0042 m. The vector in **Table 24** may be multiplied by each of the previous tables to obtain the (correlated) errors in marker positions.

Table 24: Uncertainties in fitted parameters. Changing the best fit values by these amounts result in a doubling of the RMS residual fitting error.

Parameter	Error
V_x	0.0062 m
V_x	0.0055 m
V_x	0.0038 m
θ_{CM}	2.44 10^{-6} rad
θ_{DM}	2.44 10^{-6} rad
θ_z	1.72 10^{-6} rad

3.3 Livingston Local Coordinate Systems in each station

Table 25, **Table 26** and**Table 27** present the direction cosines between the global coordinate system and the local coordinate systems for each station. The local coordinates are defined in LIGO-L950128 and LIGO-T950004 listed in **Table 1**.

Table 25: Livingston Vertex Global-Local System Direction Cosines

	$\hat{x}_L$	$\hat{y}_L$	$\hat{z}_L$
$\hat{x}_G$	1 - 4.872 10^{-8}	0	-0.000312
$\hat{y}_G$	-1.90619 10^{-7}	1 - 1.865 10^{-7}	-0.000611
$\hat{z}_G$	0.000312	0.000611	1 - 2.352 10^{-7}

Table 26: Livingston X End Station (d= 4000m) Global-Local System Direction Cosines

	$\hat{x}_L$	$\hat{y}_L$	$\hat{z}_L$
$\hat{x}_G$	1 - 4.953 10^{-8}	0	0.000315
$\hat{y}_G$	1.919 10^{-7}	1 - 1.859 10^{-7}	-0.000610
$\hat{z}_G$	-0.000315	0.000610	1 - 2.354 10^{-7}

Table 27: Livingston Y End Station (d= 4000m) Global-Local System Direction Cosines

	$\hat{x}_L$	$\hat{y}_L$	$\hat{z}_L$
$\hat{x}_G$	1 - 4.843 10^{-8}	0	-0.000311
$\hat{y}_G$	5.840 10^{-9}	1 - 1.761 10^{-10}	0.0000188
$\hat{z}_G$	0.000311	-0.0000188	1 - 4.861 10^{-8}

3.4 Positions of LIGO Primary GPS Monuments in the Global Coordinate System

The Livingston site has surveyed array of 19 primary GPS monuments. The data in **Table 28** present the SJB survey results as report on an SJB drawing, signed and dated 19 September 1997.

Table 28: Report Geodetic Coordinates for the GPS primary monuments at Livingston[a]

Monument ID	*Latitude[N]*			*Longitude[W}*			*Ellipsoidal height of marker*
	°	′	″	°	′	″	*m*
LIGO 1	30	31	47.14036	90	45	42.28956	-11.6910
LIGO 2	30	32	45.77207	90	46	3.605033	-10.4008
LIGO 3	30	33	45.57113	90	46	23.895763	-8.3971
LIGO 4	30	33	28.144005	90	47	37.33406	-8.3762
LIGO 5	30	33	9.222812	90	48	50.44142	-9.2898
LIGO 101	30	33	9.138402	90	48	46.04203	-8.8302
LIGO 103	30	33	14.283633	90	48	27.463132	-8.8923
LIGO 105	30	33	19.111329	90	48	10.039553	-9.8332
LIGO 107	30	33	23.632935	90	47	53.64897	-8.5603
LIGO 111	30	33	33.27441	90	47	18.825012	-8.9727
LIGO 113	30	33	38.39051	90	47	0.30096100	-9.4351
LIGO 115	30	33	44.88060	90	46	35.10847	-9.6865
LIGO 114	30	33	41.98956	90	46	24.553803	-9.2624

Table 28: Report Geodetic Coordinates for the GPS primary monuments at Livingston[a]

Monument ID	*Latitude[N]*			*Longitude[W}*			*Ellipsoidal height of marker*
	°	′	″	°	′	″	*m*
LIGO 112	30	33	30.714303	90	46	20.319260	-9.5362
LIGO 110	30	33	13.701668	90	46	14.055644	-9.7217
LIGO 108	30	33	0.4880430	90	46	9.226404	-10.2545
LIGO 106	30	32	29.385051	90	45	57.76082	-11.5090
LIGO 104	30	32	13.320793	90	45	51.86420	-11.5959
LIGO 102	30	31	59.20009	90	45	46.66725	-11.6330

a. SJB provided orthometric heights only; the height of the geoid relative to the WGS84 ellipsoid was calculated using the GEOID96 FORTRAN program available from the US Geodetic Survey.

Figure 7: Layout of the CB&I control points and primary GPS monument array at Livingston. Dots (colored) denote the CB&I control points for alignment of the beam tubes; plus signs denote the primary GPS monuments.

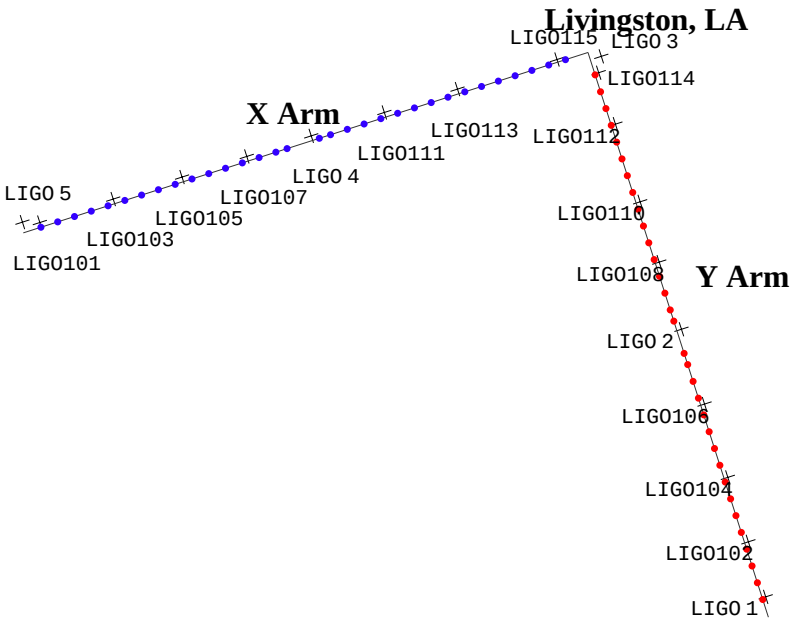

Figure 7 depicts graphically the overall site layout, including CB&I control points, beam tube centerlines and primary GPS monuments.

Table 29 presents the calculated locations of the primary GPS monuments in the site global coor-

dinate system. Dimensions are in meters.

Table 29: Position of the GPS primary monuments in the site global coordinate system

Monument ID	X_G	Y_G	Z_G
LIGO 1	-24.354011	3863.778	-3.940493
LIGO 2	-32.39879	1970.9518	-2.9398506
LIGO 3	-77.58747	52.21562	-1.8169736
LIGO 4	1950.0210	-32.30165	-1.5120938
LIGO 5	3983.322	-70.70532	-2.7601553
LIGO 101	3872.435	-32.51023	-2.2432689
LIGO 103	3352.541	-32.59589	-2.1733581
LIGO 105	2864.9596	-32.77025	-3.0290268
LIGO 107	2406.4779	-32.37370	-1.7095796
LIGO 111	1432.0647	-32.61503	-2.1331897
LIGO 113	913.8685	-32.41294	-2.6619423
LIGO 115	213.52234	-18.458987	-3.0615683
LIGO 114	-27.319999	151.94342	-2.6068115
LIGO 112	-29.160738	517.0383	-2.6774962
LIGO 110	-28.761831	1066.8928	-2.5956056
LIGO 108	-27.557296	1493.6743	-2.9534150
LIGO 106	-27.254956	2499.0584	-3.909666
LIGO 104	-26.480611	3018.1235	-3.904589
LIGO 102	-26.160749	3474.502	-3.896069

4 GRAPHICAL REPRESENTATIONS OF THE INTERFEROMETER PLANES FOR EACH SITE

Figure 8 presents graphical representations of the orientations of the interferometer planes at the two sites relative to a surface of constant elevation (referred to the vertex) from various points of view. A spherical earth was assumed in generating the pictures (deviations from geoid or ellipsoid do not affect results at the level of precision required).

Figure 8: Representation of the interferometer plane inclinations at the two LIGO sites.

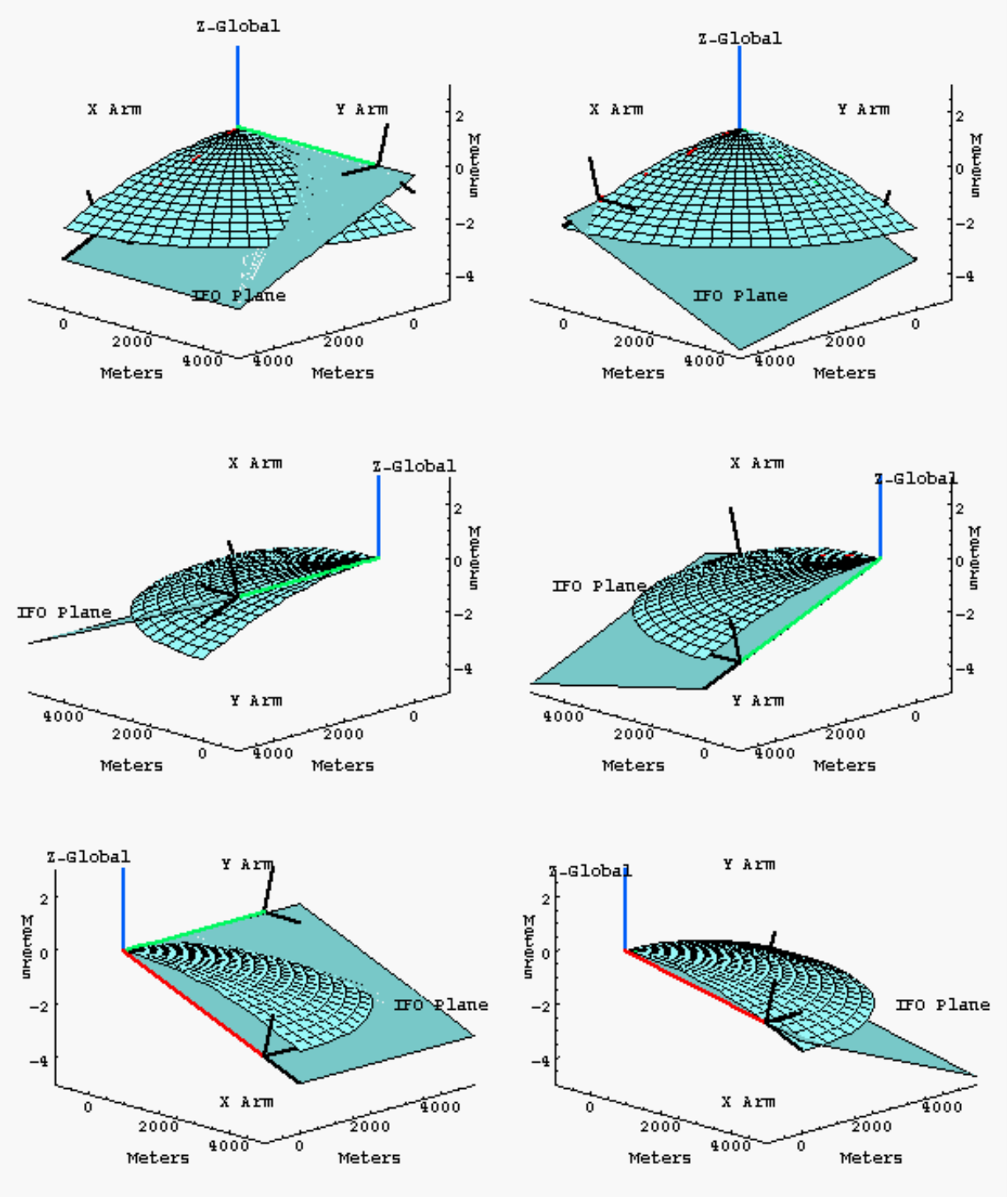

HANFORD, WA **LIVINGSTON, LA**